Int. J. Solids Structures, 1972, Vol. 8, pp. 679 to 697. Pergamon Press. Printed in Great Britain

STRUCTURAL CONSEQUENCES OF SMALL IMPERFECTIONS IN ELASTIC THIN SHELLS OF REVOLUTION

C. R. CALLADINE†

University Engineering Department, Cambridge University, Cambridge, England

Abstract—The equations of a symmetrically loaded elastic thin shell of revolution are set up in such a way that the effects of small deviations of the meridian from a "perfect" form may be analyzed with ease. Solutions are found for several kinds of imperfection and the results plotted in a specially compact form. The structural effects depend strongly on the meridional length of the imperfection. Some shell junction problems can be analyzed in terms of imperfections. The method can be extended to find classical buckling loads for axially symmetric modes.

NOTATION

A, B, C	terms in equations (24), (25)
E	Young's modulus
F	uniform outward ring load per unit circumference
H	stress resultant per unit length (Fig. 3)
K	bending stiffness of shell element [equation (14)]
L	various meridional lengths
$L(\ldots)$	Meissner's operator [equation (17)]
M	bending stress resultant per unit length (Fig. 1)
N	direct stress resultant per unit length (Fig. 1)
P	function of shell loading [equation (19)]
Q	shearing stress resultant (Fig. 1)
R	radius of (equivalent) cylindrical shell
T	thickness of shell
U	shearing force $= r_0 H$
c	number $\simeq 1{\cdot}3$, depending on value of Poisson's ratio [equation (15), Fig. 4]
e_ϕ	eccentricity of effective meridian $= M_\phi/N_\phi$
f	parameter in solution for sinusoidal imperfection [equation (39), Fig. 14]
g	attenuation factor for peak M_ϕ (Fig. 9)
l	meridional length of typical imperfection
h	"rise" of spherical cap (Fig. 5)
p	local outward normal component of surface traction per unit area
$r_{0\ldots3}$	radii defined in Fig. 2
s	meridional length co-ordinate
v	tangential component of displacement (Fig. 2)
w	normal component of displacement (Fig. 2)
β	shell parameter $= c/\sqrt{(RT)}$
γ	$= Lc/2\sqrt{(RT)}$
ε	direct strain
κ	curvature change due to bending moment
λ	equivalent length of imperfection [equation (37), Fig. 12]
ν	Poisson's ratio
ξ	deviation of meridian from perfect (Fig. 6)
σ	normal stress
χ	rotation of tangent (Fig. 2)
0 (subscript)	standard quantities (Fig. 7)

† University Lecturer in Engineering, University of Cambridge and Fellow of Peterhouse.

θ (subscript)	circumferential direction
ϕ (subscript)	meridional direction
* (superscript)	membrane solution
b (superscript)	bending
p (superscript)	perfect meridian

INTRODUCTION

THIS paper is concerned with the question of how much a small imperfection in form of a thin shell of revolution affects the distribution of stress due to an applied static loading.

Clearly an extremely slight imperfection may cause negligible deviations from the nominal or "perfect" stress distribution. On the other hand, an eccentricity of tension within an element of a plate or shell equal to only one-sixth of the thickness produces elastic "bending stress" equal in magnitude to the nominal tensile stress.

In some situations concentrations of stress due to imperfections of form are of little concern to the designer; as, for example, when the material possesses ample ductility. In other cases, notably when fatigue is an important design consideration, the effects are not negligible and should therefore be studied.

In 1955 Carlson and McKean [1] discussed the general problem of the effects of geometrical imperfections on the behaviour of pressure vessels and drew some valuable conclusions from the results of intelligent general analysis and experimental observations. They used some earlier work of Haigh [2].

Several investigators have tackled more tractable specific problems concerning imperfections in form of the meridian of a thin shell of revolution. Thus, Clark and Reissner [3] considered a slightly imperfect cylinder under axial load, Flügge [4, p. 364] studied deadweight stresses in an imperfect hemispherical shell and Steele and Skogh [5] studied the effects of slope discontinuities in axially symmetric pressure vessels.

All of these studies have involved moderately heavy analytical and/or numerical work.

The object of the present paper is to explore and present simpler and more general ways of tackling problems of the same sort. Realization of this aim is possible as a result of recent work by the author [6] which includes a simple re-statement of the classical equations of thin shells of revolution, in consequence of the definition of some useful new variables.

The calculations turn out to be gratifyingly simple and the effects of several sorts of imperfection can be assessed without difficulty. Simple general principles may be adduced and the results applied to shells of arbitrary (but sufficiently smooth) shells of revolution.

Attention is restricted to linear-elastic shells which are stress-free before the application of load. These restrictions are not unrealistic for moderately small stress-relieved pressure vessel structures, but it should be remembered that there are other situations where imperfections are inextricably associated with initial stresses and yet others where loads, e.g. self-weight, are not removable. Such problems warrant further study.

EQUATIONS OF THE PROBLEM

Equilibrium equations

Figure 1 shows positive bending, direct and shearing stress resultants per unit length of centre-surface, acting on an arbitrary small element of a symmetrically loaded shell of revolution. All stress resultants not shown vanish identically, by symmetry.

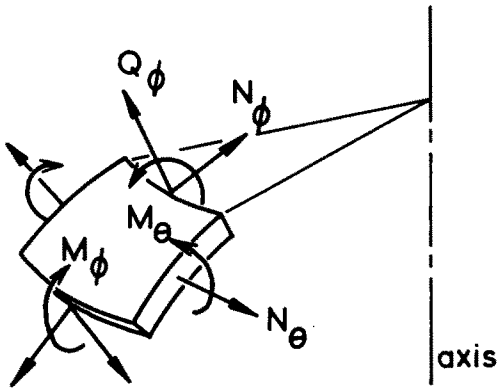

FIG. 1. Stress resultants on element of thin shell of revolution.

Figure 2 shows a portion of the meridian of an arbitrary shell of revolution. Four radii are defined at any point on the meridian: r_0 is the perpendicular distance from the axis, r_1 and r_2 are the principal meridional and circumferential radii of curvature, respectively, and r_3 is the distance from the axis, measured along the projection of the local tangent. Distance along the meridian from an arbitrary reference point is denoted by s. The symbols in Figs. 1 and 2 are in general accord with the notation of Flügge [4] and

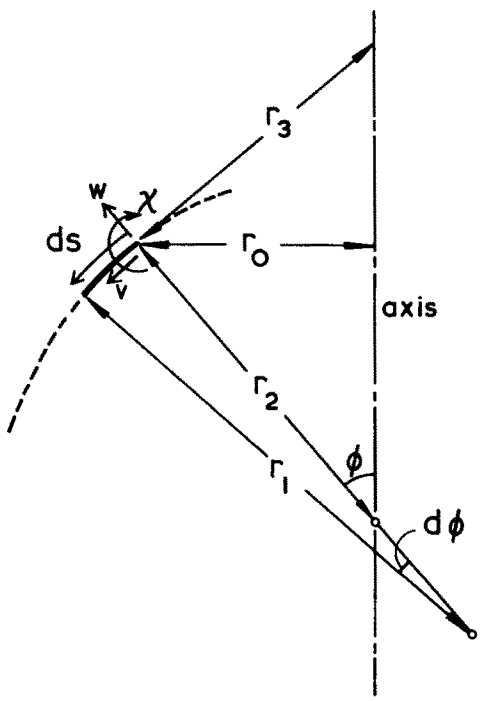

FIG. 2. Geometry of meridian and components of displacements.

Timoshenko [7]; the only novelty is the definition of r_3. All trigonometrical functions of the meridional angle ϕ are readily expressed as ratios between r_0, r_2 and r_3.

For a given shell and loading we may readily calculate the "membrane" stress resultants N_ϕ^*, N_θ^* by considerations of statical equilibrium. Since in the membrane theory $Q_\phi \equiv 0$ we may find N_ϕ^* by studying the axial equilibrium of a "cap" and then find N_θ^* from the radial equilibrium equation,

$$N_\phi^*/r_1 + N_\theta^*/r_2 = p. \tag{1}$$

where p is the local outward normal component of the surface traction per unit area.

In general, of course, the assumptions of membrane theory will not apply and we shall have instead three non-trivial equilibrium equations for the element shown in Fig. 1.

These may be written [6]

$$\frac{dU}{ds} = N_\theta^* - N_\theta \tag{2}$$

$$\frac{U}{r_3} = N_\phi^* - N_\phi \tag{3}$$

$$\frac{dM_\phi}{ds} + \left[\frac{M_\phi - M_\theta}{r_3}\right] = \frac{U}{r_2} \tag{4}$$

where

$$U = r_2 Q_\phi.$$

Equations (2) and (3) express clearly the idea that the membrane solution applies when $Q_\phi \equiv 0$.

These equations are precisely equivalent to 7(a)–(c) on p. 320 of [4] or equations (312) in [7]. They are formally simpler and the loading terms enter *indirectly*, *via* the membrane stress resultants.

Equation (3) expresses the axial equilibrium equation for a cap. Figures 3(a) and (b) show two statically equivalent ways of decomposing the force vector acting on a circumferential cut; the vector sum of H (perpendicular to the axis) and N_ϕ^* is equal to the vector sum of Q_ϕ and N_ϕ.

It follows by elementary trigonometry that

$$H = Q_\phi \operatorname{cosec} \phi$$

hence

$$U = r_2 Q_\phi = r_0 H. \tag{5}$$

Thus U is the total shearing force across a radius, as shown in Fig. 3(c).

Kinematic equations

It is again advantageous to use r_3 in setting up the kinematic equations for the shell. Let w and v be component small displacements of a point on the meridian in directions normal and tangential to the meridian, respectively, and let χ be a small rotation of the meridian, as shown in Fig. 2. Then if κ_ϕ, κ_θ are the principal curvature changes and ε_ϕ, ε_θ

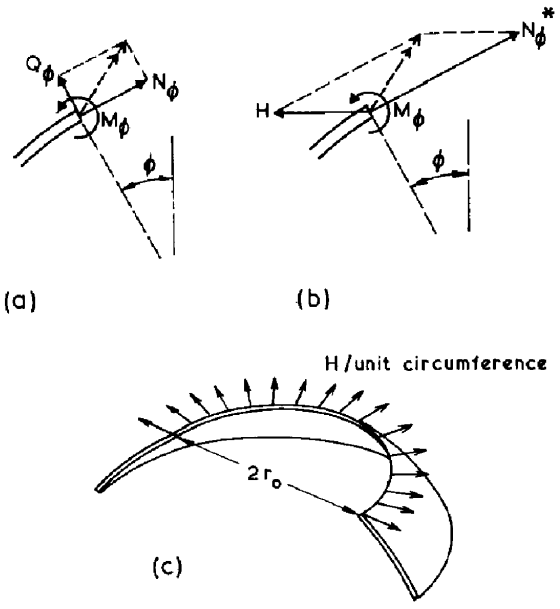

FIG. 3. Aspects of shearing stress resultant.

the changes in in-plane strain due to v, w and χ, it follows simply that

$$\varepsilon_\phi = \frac{dv}{ds} + \frac{w}{r_1}, \qquad \varepsilon_\theta = \frac{v}{r_3} + \frac{w}{r_2}, \qquad \chi = \frac{dw}{ds} - \frac{v}{r_1} \tag{6}$$

$$\kappa_\phi = \frac{d\chi}{ds} \tag{7}$$

$$\kappa_\theta = \frac{\chi}{r_3}. \tag{8}$$

In these equations various negligible terms have been omitted, following [4, chapter 6]. Further, v and w may be eliminated from (6) to give the compatibility relation

$$\frac{d\varepsilon_\theta}{ds} + \left[\frac{\varepsilon_\theta - \varepsilon_\phi}{r_3}\right] = \frac{\chi}{r_2}. \tag{9}$$

The form of (7)–(9) and (2)–(4) is similar, save for the lack of "loading" terms in (7) and (8): i.e. the well-known static-geometric analogy [8] holds.

Elastic constitutive relations

In elastic analysis of initially stress-free shells, we couple (2)–(4) and (7)–(9) by means of constitutive relations between the strain and stress resultants for an element of shell. Let E be Young's modulus and ν Poisson's ratio for the material and let T be the (constant)

thickness of the shell; then the relations we seek are

$$M_\phi = K(\kappa_\phi + \nu\kappa_\theta) \tag{10}$$

$$M_\theta = K(\kappa_\theta + \nu\kappa_\phi) \tag{11}$$

and

$$\varepsilon_\theta = (N_\theta - \nu N_\phi)/ET \tag{12}$$

$$\varepsilon_\phi = (N_\phi - \nu N_\theta)/ET. \tag{13}$$

The bending stiffness, K, is given by

$$K = ET^3/4c^4 \tag{14}$$

where

$$c = (3(1-\nu^2))^{\frac{1}{4}}. \tag{15}$$

Figure 4 shows c as a (rather insensitive) function of ν. These relations embody the assumption that no deformation is attributable directly to Q_ϕ, which is reasonable for sufficiently thin shells [4]. Putting (4) in terms of χ by using (10), (11), (7) and (8), we find

$$L(\chi) - \left[\frac{\nu\chi}{r_1}\right] = \frac{U}{K} \tag{16}$$

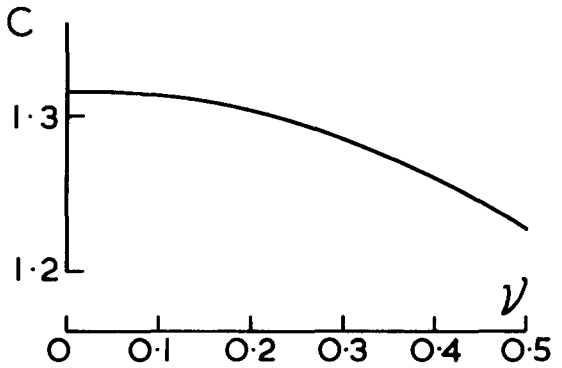

FIG. 4. Variation of parameter c with Poisson's ratio.

where the operator $L(\ldots)$ is given by

$$L(\ldots) = r_2\left(\frac{d^2}{ds^2}(\ldots) + \frac{1}{r_3}\frac{d}{ds}(\ldots) - \frac{1}{r_3^2}(\ldots)\right). \tag{17}$$

Similarly, putting (9) in terms of U we have

$$L(U) + \left[\frac{\nu U}{r_1}\right] = Pr_2 - \chi ET \tag{18}$$

where

$$P = \frac{dN_\theta^*}{ds} - \nu\frac{dN_\phi^*}{ds} + \left[\frac{(1+\nu)}{r_3}(N_\theta^* - N_\phi^*)\right]. \tag{19}$$

Operator $L(\ldots)$, Meissner's operator, is well known in elastic shell analysis (see [4, p. 360]), but its present "clean" form is due to the introduction of r_3 as a variable. For a cylindrical shell $r_3 \to \infty$ and the second and third terms of $L(\ldots)$ vanish.

Simplifying the equations

In many practical problems the operator $L(\ldots)$ can be simplified in consequence the observation, due to Geckeler [9], that the omission of the second and third terms, together with the second terms on the left hand side of (16) and (18), has little effect upon the solution. When this is so the equations are analogous to those of a cylindrical shell (for which $r_3 \to \infty$), and the "boundary layer" due to a discontinuity extends a meridional distance of order $\sqrt{(r_2 T)}$.

The second and third terms of $L(\ldots)$ may be dropped if

$$\sqrt{(r_2 T)} \ll r_3. \tag{20}$$

In any given case the relative magnitudes of r_3 and $\sqrt{(r_2 T)}$ may be determined by inspection. At the edge of a cap of a spherical shell, for example, we find by simple geometry that

$$\frac{r_3}{\sqrt{(r_2 T)}} > \sqrt{\left(\frac{2h}{T}\right)}$$

where h is the "rise" of the cap: see Fig. 5. Calculations show that if $r_3/\sqrt{(r_2 T)} > 5$, i.e. if the rise of the cap is more than about 10 times the thickness, it is safe to use the simplified form of $L(\ldots)$. We would arrive at the same resulting equations by neglecting the terms in square brackets in (4) and (9).

In the remainder of this paper we shall assume that the Geckeler approximation is justified, so our analysis will not be applicable to a limited region near the crown of a spherical shell.

SHELLS HAVING IMPERFECT MERIDIANS

Effect on the membrane stress resultants

Our first task in studying the consequences of an imperfection in the meridian is to find the effect of the imperfection on the membrane stress resultants N_θ^* and N_ϕ^*, which appear in the loading term of the general equations.

Let the small deviation of the meridian from the "perfect" meridian be expressed as $\xi(s)$, measured normal to the perfect meridian as shown in Fig. 6. Denoting changes due to the introduction of the imperfection by the operator Δ, we find, by differentiating (1):

$$\Delta N_\phi^*/r_1 + N_\phi^* \Delta(1/r_1) + \Delta N_\theta^*/r_2 + N_\theta^* \Delta(1/r_2) = 0. \tag{21}$$

We need therefore to find $\Delta(1/r_1)$ and $\Delta(1/r_2)$ in terms of $\xi(s)$. By geometry

$$\Delta(1/r_1) \simeq d^2\xi/ds^2 \tag{22}$$

$$\Delta(1/r_2) \simeq -(d\xi/ds)/r_3 - \xi/r_2^2. \tag{23}$$

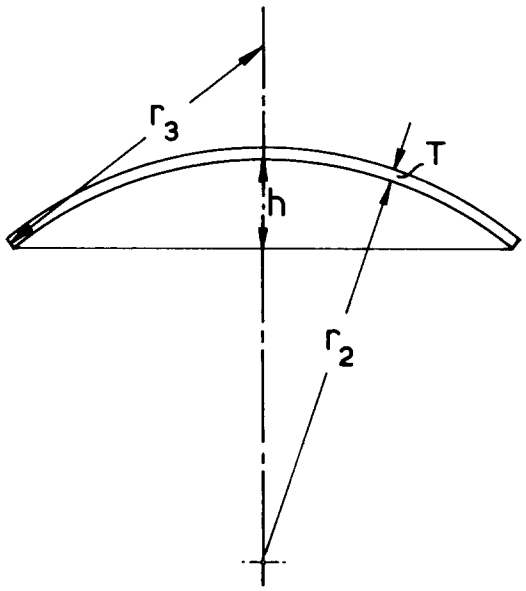

FIG. 5. Geometry of a spherical cap.

Let us examine the relative magnitudes of these terms by considering an imperfection of the form

$$\xi = (\xi_0/2)(1-\cos 2\pi s/l)$$

where the origin for s is at one end of the imperfection, whose meridional extent is l. Further (anticipating a later result), we take $\sqrt{(r_2 T)}$ as a typical value of l. Putting peak values of the derivatives in (22) and (23) we have

$$\Delta(1/r_1) = 2\pi^2 \xi_0 / r_2 T = A \tag{24}$$

$$\Delta(1/r_2) = (\pi \xi_0 / r_3 \sqrt{(r_2 T)}) + (\xi_0 / r_2^2) = B + C. \tag{25}$$

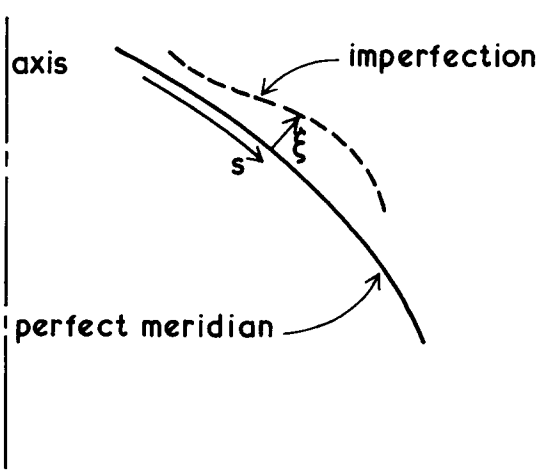

FIG. 6. Specification of an imperfection.

Now C/A has the same order of magnitude as $T/10r_2$, which is small for thin shells, and B/A has the same order of magnitude as $\sqrt{(r_2T)}/6r_3$, which is also small since we are assuming $r_3/\sqrt{(r_2T)} > 5$. Consequently we may put

$$\Delta(1/r_2) \ll \Delta(1/r_1). \tag{26}$$

Thus the meridional curvature is much more sensitive than the circumferential curvature to the presence of an imperfection of this sort. This result is stronger the smaller the value of l.

The membrane equilibrium equation for a "cap" may be written

$$N_\phi^* . 2r_0^2/r_2 = \text{axial load on cap}$$

where the right hand side includes the effect of all forces and pressures. Differentiating, as before, we have

$$\Delta N_\phi^*/r_2 + N_\phi^* \Delta(1/r_2) = 0.$$

In this equation changes in r_0, which affect the left hand side (and right hand side when there is pressure loading) have been neglected, since $\Delta r_0/r_0 = \xi/r_2$, which is small compared to the terms retained.

Putting $r_3 = 10\sqrt{(r_2T)}$, for example [see (20)], and $\xi_0 = T/3$ we find from (25)

$$r_2\Delta(1/r_2) \doteq 0{\cdot}1.$$

Hence it seems reasonable to neglect changes in r_2 altogether, i.e. to put $\Delta(1/r_2) = 0$. We thus obtain, from (26), (21) and (22)

$$\Delta N_\phi^* = 0 \tag{27}$$

$$\Delta N_\theta^* = r_2 N_\phi^* \, \mathrm{d}^2\xi/\mathrm{d}s^2. \tag{28}$$

This somewhat brutal set of approximations turns out very well in practice. In his example Flügge [4, p. 364] points out that N_ϕ^* for the imperfect shell is virtually indistinguishable from that for the perfect shell, while in contrast N_θ^* fluctuates wildly: it is, indeed, given almost exactly by (28). Also, Heyman [10] has pointed out that small adjustments in the meridional profile of domes can result in large changes in N_θ^* with, nevertheless, negligible changes in N_ϕ^*.

We now suppose that the meridional shape and loading of the "perfect" shell are such that the actual and the membrane stress resultants differ negligibly. Then the membrane stress resultants for the imperfect shell are given by

$$N_\theta^* = N_\theta^p + N_\phi^p r_2 \, \mathrm{d}^2\xi/\mathrm{d}s^2 \tag{29}$$

$$N_\phi^* = N_\phi^p \tag{30}$$

where superscript p denotes the perfect shell.

To study the effects of a given imperfection we can solve (16) and (18) simultaneously. Substituting (29) and (30) in (19) we find, after neglecting small terms:

$$P = N_\phi^p r_2 \, \mathrm{d}^3\xi/\mathrm{d}s^3. \tag{31}$$

We shall consider first shells having perfect meridians with $r_2 = \text{const.} = R$. Again neglecting changes in r_2 due to the imperfection and using the Geckeler approximation,

we find that the left hand side of (16) and (18) are unchanged by the introduction of the imperfection, so the equations are particularly easy to solve.

A physical interpretation

In many situations it is useful to think in terms of the physical meaning of equations. In our equations, as we have seen, the imperfection enters only on the right hand side, via the computation of N_θ^*. Thus the solution for the effect of the imperfection is precisely as for a perfect cylindrical shell of radius R loaded by pressure varying along the meridian in such a way that N_θ^* is the same as in the imperfect shell. This distribution of internal gauge pressure on the perfect shell corresponding to the effect of the imperfection is given by

$$p = N_\phi^p \, \mathrm{d}^2\xi/\mathrm{d}s^2 \tag{32}$$

which has an obvious physical interpretation. Further, if there is a slope discontinuity $[\mathrm{d}\xi/\mathrm{d}s]$, we have a corresponding line load per unit circumference of intensity

$$F = N_\phi^p[\mathrm{d}\xi/\mathrm{d}s]. \tag{33}$$

Now for a line load F per unit length acting on a cylindrical shell of radius R and thickness T the distributions of N_θ and M_ϕ are symmetrical about the plane $s = 0$ of the load, and are given for $s > 0$ by the equations [7, p. 471]

$$\left.\begin{aligned} N_\theta &= (Fc\sqrt{R}/2\sqrt{T})\,\mathrm{e}^{-\beta s}(\cos\beta s + \sin\beta s) \\ M_\phi &= -(F\sqrt{(RT)}/4c)\,\mathrm{e}^{-\beta s}(\cos\beta s - \sin\beta s) \end{aligned}\right\} \tag{34}$$

where

$$\beta = c/\sqrt{(RT)}.$$

These relations are plotted in Fig. 7.

Hence, for any arbitrary imperfection profile we can find the corresponding distributions of N_θ and M_ϕ by working out p and F according to (32) and (33) and then suitably superposing multiples of the symmetrical standard distributions (34).

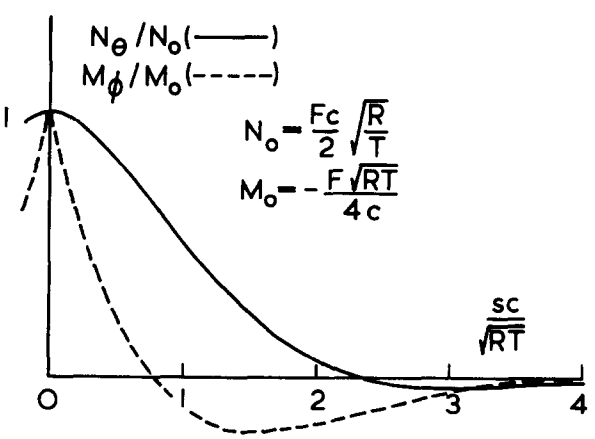

FIG. 7. Stress resultants for cylindrical shell carrying a ring load.

EXAMPLES OF IMPERFECTIONS

Simple slope discontinuity

The simplest imperfection to study is a slope change in the meridian, as when a cylindrical shell is joined onto a conical shell with a slight taper. (Discontinuities of this sort occur in some finite-element representations of shells of revolution [11].) For a slope discontinuity of $[d\xi/ds]$ (34) may be used directly with (33).

It is interesting to plot the results in a way suggested by Flügge to show the magnitude of M_ϕ relative to N_ϕ. Let $e_\phi = M_\phi/N_\phi$ be the eccentricity of the meridional tension statically equivalent to M_ϕ and N_ϕ together. The eccentricity may easily be plotted, as in Fig. 8, together with the meridian itself, to an arbitrary scale. By (34)

$$e_\phi^{\max} = [d\xi/ds]\sqrt{(RT)}/4c. \tag{35}$$

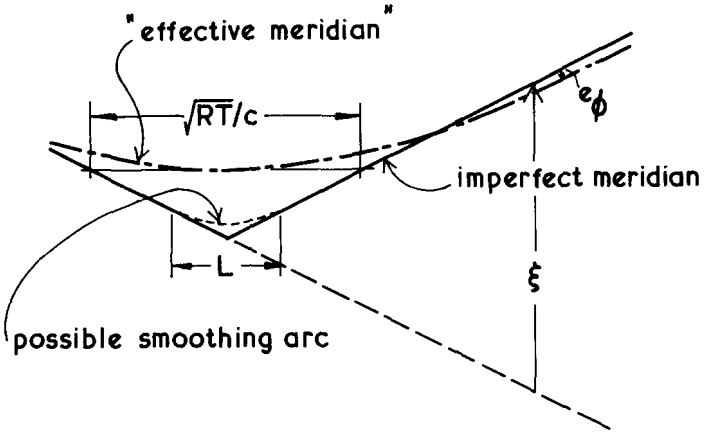

FIG. 8. Results for a slope discontinuity.

This has the geometrical interpretation shown. Note that this "eccentricity line" has no slope discontinuity: this is no accident, since by equilibrium

$$F = [dM_\phi/ds].$$

The "eccentricity line" has a useful property by virtue of the equilibrium equations (2) and (4). Omitting the term in square brackets from (4) and putting $r_2 = R$ we find, in general,

$$\begin{aligned} N_\theta &= N_\theta^* - R\,d^2M_\phi/ds^2 \\ &= N_\theta^* - RN_\phi^*\,d^2\,e_\phi/ds^2 \qquad \text{(assuming } N_\phi^* = \text{const.)} \\ &= N_\theta^p + RN_\phi^*\,d^2(\xi - e_\phi)/ds^2. \end{aligned} \tag{36}$$

Therefore, by (29) N_θ is the *membrane* stress resultant for an artificial shell whose meridian is the "eccentricity line"; see Fig. 8.

Thus for any given imperfection the complete solution (M_ϕ, N_θ) may be expressed compactly by a diagram showing the "eccentricity line". From now on we shall call this the "effective meridian" and all of our results will be plotted in this way.

Returning to the problem, let us find the peak stress in the shell wall in the ϕ direction due to bending moment M_ϕ, say σ_ϕ^b. Since for linear-elastic material

$$\sigma_\phi^b = 6M_\phi/T^2$$

we find

$$\sigma_\phi^b T/N_\phi = 6e_\phi^{\max}/T = (1{\cdot}5/c)(R/T)^{\frac{1}{2}}[\mathrm{d}\xi/\mathrm{d}s].$$

Supposing we decide, somewhat arbitrarily, that we can only tolerate a 20 per cent increase in σ_ϕ due to bending stress on account of a "kink" imperfection, we have, for $\nu \doteq 0{\cdot}3$,

$$[\mathrm{d}\xi/\mathrm{d}s] < 0{\cdot}17(T/R)^{\frac{1}{2}}.$$

Thus, for $R/T = 50$, $[\mathrm{d}\xi/\mathrm{d}s] < 0{\cdot}024$, i.e. about $1{\cdot}4°$.

In general we could tolerate higher-angle kinks with no further penalty in bending stress if we could "round" the kink by a faired parabola extending a meridional distance L, as indicated in Fig. 8. By our previous analysis this gives an attenuation effect exactly as if the equivalent ring load F were uniformly spread as a pressure over a meridional length L. The attenuation factor for peak M_ϕ is readily computed [7] to be

$$g = \mathrm{e}^{-\gamma} \sin \gamma/\gamma$$

where

$$\gamma = Lc/2\sqrt{(RT)},$$

and this is plotted in Fig. 9. Using this curve we can work out the relation between L and $[\mathrm{d}\xi/\mathrm{d}s]$ resulting in our tolerable 20 per cent bending stress and this is shown in Fig. 10.

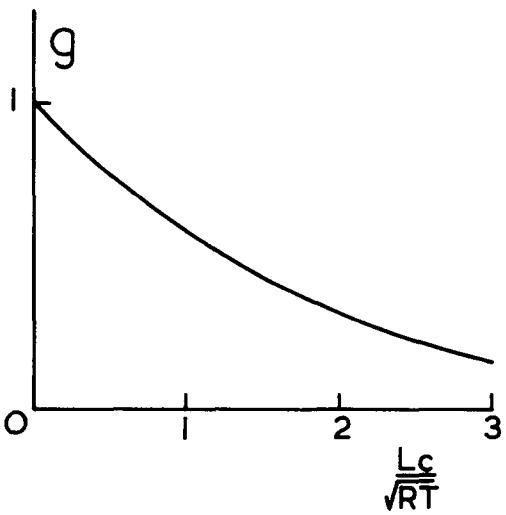

FIG. 9. Attenuation of peak M_ϕ when a ring load is spread over a length L.

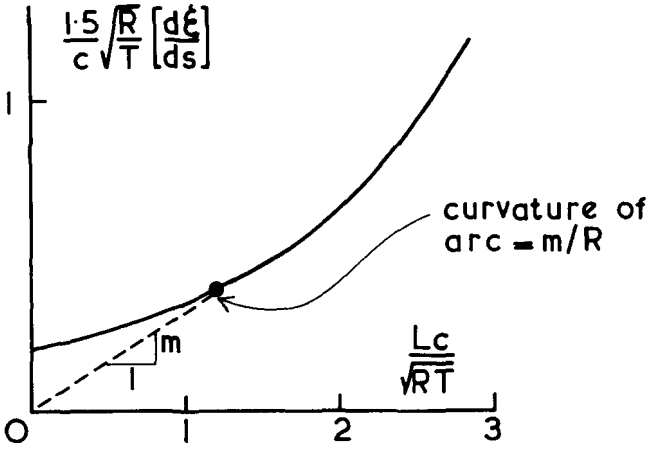

FIG. 10. Increase in slope discontinuity tolerable when a smoothing arc is inserted.

The meridional curvature of the "bridging arc" is given by the construction shown, for any point on the curve.

Another useful result is that for $Lc/\sqrt{(RT)} \leq 0{\cdot}5$, approximately, the location of the "effective meridian" is virtually unchanged by the insertion of the smoothing section.

An isolated "bump"

Calculations of the effective meridian for a class of imperfections involving a "blip" in the meridian are shown in Fig. 11 for three different lengths of imperfection. The imperfection profiles range from one corresponding to a stress-relieved "weld sinkage" to an alignment imperfection of a strake. For corresponding curves, the horizontal scale for all profiles is the same, as indicated. It turns out to be useful to define an effective length λ as follows:

$$\lambda = \int_0^L \xi \, ds/\xi_0. \tag{37}$$

Thus imperfections having the same height and area included beyond the perfect meridian, like those shown, have the same value of λ. The advantage of using λ is that for $\lambda c/\sqrt{(RT)} \leq 1{\cdot}2$, approximately, the effective meridian is virtually independent of the details of the imperfection profile, as may be verified by inspection of Fig. 11. For higher values of λ the effective meridians differ from each other, since each approximates the imperfection profile more closely as λ increases. The points marked on the curves for $\lambda c/\sqrt{(RT)} = 3{\cdot}69$ were found by using the construction of Fig. 8 at each discontinuity of slope.

More results are plotted in Fig. 12, which shows how the peak eccentricity at the effective meridian varies with the length of the imperfection. The diagram illustrates the previous remarks. The fact that the slope discontinuities may be considered separately for the longer wavelengths justifies our earlier step of taking $\sqrt{(r_2 T)}$ as a typical length of imperfection.

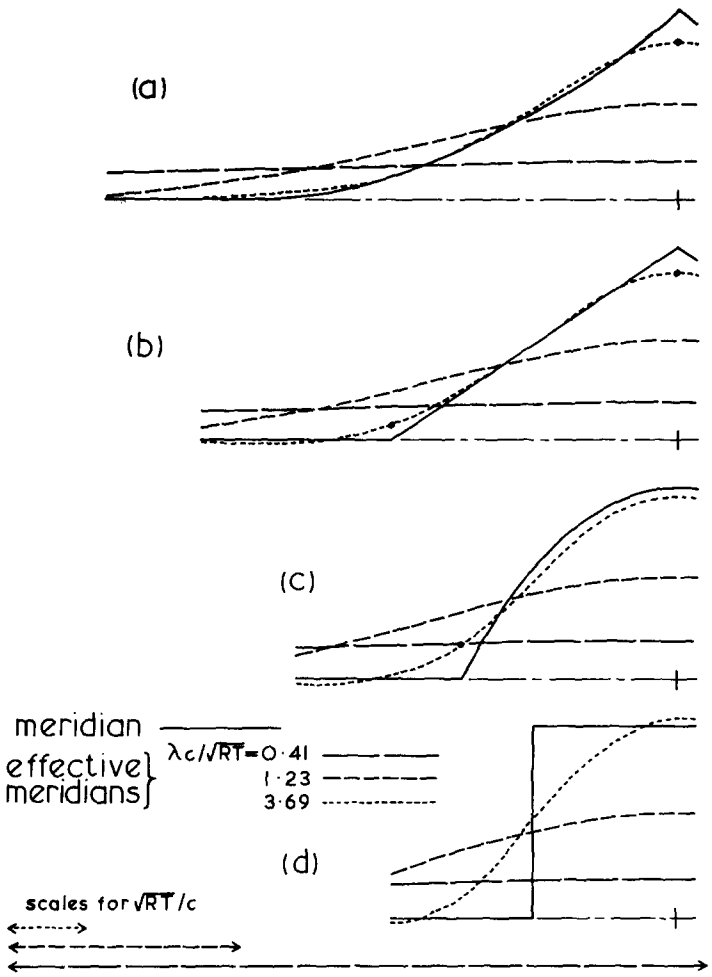

FIG. 11. Results for various symmetrical imperfections.

The results of these calculations agree very well with those of Steel and Skogh [5], who studied imperfections of the types shown in Fig. 11(a) and also a range of more acute imperfection shapes made from higher degree parabolas.

The imperfection studied by Flügge [4, p. 364] is very similar to that of Fig. 11(c) except that the slope discontinuities were "rounded" over a meridional length $\simeq 0{\cdot}59\ \sqrt{(RT)}/c$. This should not have much effect on the effective meridian, as argued above. In our notation Flügge had $Lc \simeq 4{\cdot}3\ \sqrt{(RT)}$ and the resulting effective meridian (not shown) is virtually identical to Flügge's results. It should be noted that in [4] N_ϕ^* varies by about 13 per cent from one end of the imperfection to the other. Our method of plotting minimizes the consequence of this.

Antimetric imperfections

Figure 13 shows results for two antimetric imperfections, involving a smoothed step in the meridian. The same scheme of plotting applies as to Fig. 11 and again we find that

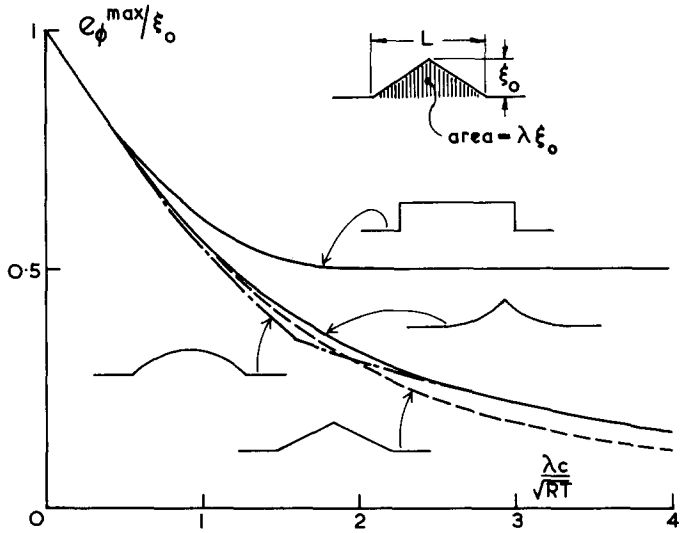

FIG. 12. Peak eccentricity of effective meridian for various symmetrical imperfections.

for the same λ [defined by (37) for the corresponding *symmetric* imperfection] the effective meridian is insensitive to the details of the imperfection profile for $\lambda c/\sqrt{(RT)} \leq 1{\cdot}2$. For higher values of λ the effective meridian follows more closely the form of the imperfection, with slope discontinuities behaving separately, as before.

Periodic imperfections

Clark and Reissner [3] studied the behaviour of nearly-cylindrical shells with undulating meridians under uniform axial loading.

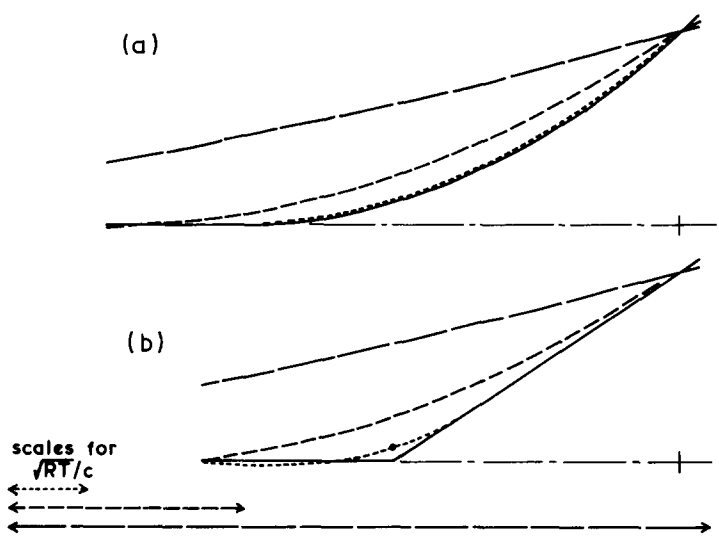

FIG. 13. Results for various antimetric imperfections.

This kind of problem is readily analyzed by the methods of the present paper. For example, let the meridian profile be

$$\xi = \xi_0 \sin \pi s/L \tag{38}$$

where L is the half-wave length. Then putting $N_\phi^* = -N_0$ we obtain

$$N_\theta^* = N_0 \xi_0 (\pi^2/L^2) \sin \pi s/L.$$

Substituting into (19) and solving (16) and (18) subject to distant boundary conditions, we find

$$M_\phi = -f\xi N_0, \qquad N_\theta = (1-f)N_\theta^* \tag{39}$$

where

$$f = \{1+(4/\pi^4)(Lc/\sqrt{(RT)})^4\}^{-1}. \tag{40}$$

This is plotted in Fig. 14. These results indicate that the effective meridian is similar to the actual meridian but with amplitude multiplied by $(1-f)$. Thus for short waves the effective meridian is nearly straight and the bending stresses may be appreciable, while for long waves the solution approaches the membrane solution, as indeed we would expect from the previous analysis. These results agree precisely with those of [3] for sinusoidal meridians.

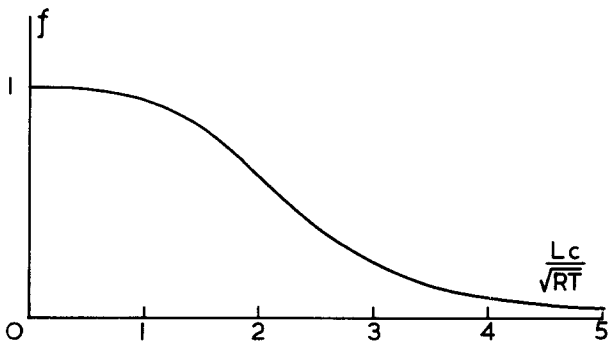

FIG. 14. Effect of wavelength on behaviour for sinusoidal imperfections.

Step change of meridional curvature

For a final example we consider an imperfection in which there is a discontinuity in meridional curvature, $\Delta(1/r_1)$, as shown in Fig. 15. The effective meridian, as computed, is also shown and, as in Fig. 8, there is a unique natural scale to the diagram. By symmetry the eccentricity is zero at the point of curvature change and has peak value $0{\cdot}0807\Delta(1/r_1)RT/c^2$ at distance $\pm 0{\cdot}785\sqrt{(RT)}/c$ from this point.

This "imperfection" corresponds, for example, to the junction between a cylindrical shell and a matching spherical cap. In this case $\Delta(1/r_1) = 1/R$ and we find that the maximum meridional bending stress is given by

$$\sigma_\phi^b T/N_\phi = 0{\cdot}484/c^2. \tag{41}$$

This result is independent of R/T and agrees exactly with an example of Flügge [4, p. 342].

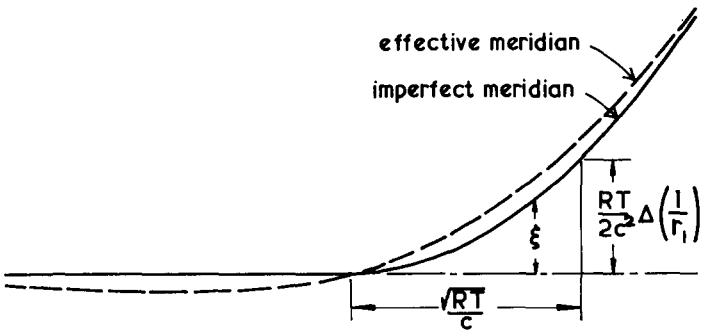

FIG. 15. Result for step change in meridional curvature.

CLASSICAL (EIGENVALUE) BUCKLING THEORY

We can readily use our methods to study classical (eigenvalue) buckling of shells of revolution. Suppose an initially perfect cylindrical shell is buckling symmetrically under $N_\phi^* = -N_0$. The current deflected meridian, say $w = w_0 \sin \pi s/L$, gives additional membrane stress resultant N_θ^*, according to (29), with $\xi = w$, which in turn "loads" the perfect shell, according to (32). The N_θ response is given by (39) and the corresponding change in radial deflection, RN_θ/ET, is simply equal to w.

The resulting equation, from which w cancels, gives the following expression:

$$N_0 = \frac{L^2}{(1-f)} \frac{ET}{R^2\pi^2}.$$

N_0 has a minimum value, $N_0 = ET^2/Rc^2$, which is therefore the classical elastic buckling load, when $Lc/\sqrt{(RT)} = \pi/\sqrt{2}$.

This result agrees with buckling formulas to be found in the classical texts (see, e.g. Timoshenko and Gere [12]) for axisymmetric buckling of cylindrical shells under end load alone or end load combined with external pressure.

The absence of N_θ^* from the buckling formulas is due simply to the fact that the equivalent change in pressure loading corresponding to an imperfection does not involve N_θ^*: see (32).

DISCUSSION

So far we have considered only shells in which r_2 is constant, i.e. cylindrical and spherical shells. It is clear, however, that our results should be applicable to other sorts of shell, e.g. conical, for which r_2 might vary by not more than a few per cent in the vicinity of an imperfection.

This raises the question of what limits, if any, there are to the meridional form of the "perfect" shell. The essence of perfection, in this context, is that there should exist practically no bending stresses. Therefore we could not, for example, consider an ASME standard torispherical pressure vessel head as perfect. Indeed, we might be tempted to regard such a head as the imperfect version of an unknown "perfect" closure.

It is clear from one of our examples that a modest step change in meridional curvature, such as from a cylindrical vessel to a hemispherical closure, can cause bending stresses of the order of 30 per cent of the nominal meridional stress. To reduce bending stresses appreciably we must either restrict abrupt changes in curvature to small fractions of the circumferential curvature or avoid step changes in curvature altogether.

When we examine the normal fabrication procedures for actual shell structures, it seems unrealistic to be sanguine about the possibility of controlling the rate of change of curvature along the meridian. Indeed, it seems clear than an initial over-pressure test may well afford the only practical means of making appropriate fine adjustments to the profile, by virtue of plastic flow. The details of such adjustments could be studied by means of relatively simple extensions of the present methods, given the appropriate material properties.

Although we set out to study the effect of "small imperfections" in shape of meridians, it is tempting to speculate that the same methods could be applied to gross imperfections such as major discontinuities in pressure vessels. Unfortunately the present results cannot be applied directly, since there are usually marked discontinuities in both N_ϕ^* and r_2 at such intersections. Further, the "effective meridian" concept, if applicable at all, would have to be re-worked carefully. However, some simple techniques for dealing with major discontinuities have already been discussed [6] and the present paper is in effect an extension of this previous work appropriate to the special circumstances of small imperfections.

SUMMARY AND CONCLUSIONS

1. Sufficiently far from the apex of a thin elastic shell of revolution with a smooth meridian [say $r_3 > 5\sqrt{(r_2 T)}$] the effect on the governing equations of introducing a small imperfection in the meridian is merely to alter the right hand side. Consequently the effects of such imperfections may be studied in isolation and general results obtained.

2. In general the effects of imperfections are most marked in terms of changes in N_θ and M_ϕ, with relatively little change in N_ϕ and they can be discussed without specific reference to the shape of the shell or the type of loading.

3. The most convenient way of presenting results is in terms of the *effective meridian.* The *membrane* stress resultant N_θ^* in a shell made in the form of the effective meridian is the same as N_θ in the imperfect shell and M_ϕ is given by N_ϕ multiplied by the separation between the actual and effective meridians.

4. The effective meridian is smooth and its form is always a smoothed-out version of the imperfect meridian. It follows closely smooth imperfections having characteristic length long compared to $\sqrt{(r_2 T)}$ but takes a fairly straight "middle" path for short imperfections.

5. A useful by-product of the analysis is the idea that some types of shell intersections may be considered as simple imperfections. The analysis also throws light on some aspects of classical buckling formulae for thin shells of revolution.

Acknowledgements—This work was begun at Stanford and finished at Cambridge. I thank the University of Cambridge for a grant of sabbatical leave and Stanford University for its hospitality.

REFERENCES

[1] W. B. CARLSON and J. D. MCKEAN, Cylindrical pressure vessels: Stress systems in plain cylindrical shells and in plain and pierced drumheads. *Proc. Inst. Mech. Engrs* **169**, 269–284 (1955).
[2] B. P. HAIGH, An estimate of the bending stresses induced by pressure in a tube that is not quite circular Appendix IX, Welding research committee 2nd report. *Proc. Inst. Mech. Engrs* **133**, 96–98 (1936).
[3] R. A. CLARK and E. REISSNER, On axially symmetric bending of nearly cylindrical shells of revolution. *J. appl. Mech.* **23**, 59–67 (1956).
[4] W. FLÜGGE, *Stresses in Shells*. Springer-Verlag (1960).
[5] C. R. STEELE and J. SKOGH, Slope discontinuities in pressure vessels. *J. appl. Mech.* **37**, 587–595 (1970).
[6] C. R. CALLADINE, Creep in Torispherical Pressure Vessel Heads, *Proc. IUTAM Symp. on Creep in Structures*, Gothenburg (1970). Springer-Verlag (to be published).
[7] S. P. TIMOSHENKO and S. WOINOWSKI-KRIEGER, *Theory of Plates and Shells*, 2nd edition. McGraw-Hill (1959).
[8] A. L. GOL'DENVEIZER, *Theory of Elastic Thin Shells*. Pergamon Press (1961).
[9] J. W. GECKELER, *Forschungsarb*, No. 276 (1926); see [7, p. 548].
[10] J. HEYMAN, On shell solutions for masonary domes. *Int. J. Solids Struct.* **3**, 227–241 (1967).
[11] P. E. GRAFTON and D. R. STROME, Analysis of axi-symmetric shells by the direct stiffness method. *AIAA Jnl* **1**, 2342–2347 (1963).
[12] S. P. TIMOSHENKO and J. M. GERE, *Theory of Elastic Stability*, 2nd edition. McGraw-Hill (1961).

(*Received* 12 *April* 1971; *revised* 28 *October* 1971)

Абстракт—Выводится уравнения для симметрически нагруженной упругой, тонкой оболочки, таким образом, чтобы можно легко аналиризовать эффекты малых отклонений меридиана от "идеальной" формы. Даются решения для некоторых случаев неправильностей. Результаты составлены в специально компактной форме. Конструкционные эффекты, в большой степени, зависят от меридионамной длины неправильностей. Некоторые задачи соединенных оболочек можно рассматривать в зависимости от неправивольности формы. Метод можно обобщить, с целью определения классической нагрузки выпучивания, для осе-симметрических видов выпучивания.